ELSEVIER

Catalysis Today 25 (1995) 357–363

CATALYSIS TODAY

# Pressure drop membrane reactor equilibrium analysis

H.W. Deckman [a,*], E.W. Corcoran [a], J.A. McHenry [a], J.H. Meldon [b], V.A. Papavassiliou [a]

[a] *Exxon Research & Engineering, Corporate Research, Annandale, NJ 08801, USA*

[b] *Chemical Engineering Department, Tufts University, Medford, MA 02155, USA*

**Abstract**

An analysis is performed for predicting conversion in membrane reactors with pores both catalytically active and so narrow that intrapore transport is in the Knudsen regime. The analysis is illustrated for A = B + C (e.g., dehydrogenation) stoichiometry, and for the limiting case of very fast, reversible reactions —i. i.e., large Thiele modulus. Thus, local concentrations are calculated from an equilibrium relationship. 'Supra-equilibrium' conversion is predicted. However, a distinction is drawn between effects attributable to permselective properties of the membrane and those simply required by le Chatelier's principle. This analysis of conversion in a catalytic membrane reactor allows the influence of intrinsic membrane properties (such as diffusivity differences) to be separated from those of extrinsic factors (such as differences in trans-membrane pressure and dilution of products in a sweep gas which may be flowing on the permeate side of the membrane). Furthermore, external mass transfer resistance, heretofore generally neglected, is examined from a multicomponent diffusion approach.

## 1. Introduction

Recently [1–8], there has been great interest in membrane reactor architectures which carry out gas-phase reactions within the pore structure of a permselective inorganic membrane impregnated with a catalyst. In this membrane reactor architecture, reactants are fed from one side of the membrane and product species and unconverted reactants are removed from the other side of the membrane. Particular attention has been given to the possibility of overcoming equilibrium limits in dehydrogenation reactions [1–3] which have the form:

$$A = B + C \qquad (I)$$

with A and B being hydrocarbon species (e.g. ethane and ethylene) and C being hydrogen.

Among the products of dehydrogenation reactions, the smaller hydrogen molecule has the highest diffusivity in both micro-and meso-pores which can be present in different types of permselective inorganic membrane materials. At the pressures and temperatures needed to conduct dehydrogenation reactions [9], hydrogen is selectively transported by a Knudsen diffusion mechanism [10] through meso-pores which have sizes greater than 20 Å and less than ca. 1000 Å. In smaller micro pores, (less than 20 Å), hydrogen can be very selectively transported with a diffusion coefficient less than that for larger sized meso-pores. In either case, hydrogen diffuses faster through the membrane pore structure than other reaction species, and as its partial pressure

* Corresponding author.

*SSDI* 0920-5861(95)00108-5

decreases the equilibrium of the reaction can be shifted to form more product.

The exact concentration profiles of each species along the pore are determined by their partial pressures at the boundaries of the membrane, their diffusion coefficients, any partitioning (such as solubility and mass transfer resistance effects) at the boundaries of the membrane, and reaction kinetics. At the high temperatures ($>300°C$) required for dehydrogenation of small paraffins ($C_2$–$C_6$, the partitioning effects at the boundaries of the membrane come primarily from external mass transfer resistance effects. Finite mass transfer rates across the gas boundary layer separating the membrane surface from the bulk of a flowing gas stream reduce the fluxes across the membrane and may limit its selectivity. The importance of this effect has been overlooked in previous models [1–4] which contain many of the physical processes within the membrane reactor but assume no external mass transfer limitations. These models have been based on integrating the material and energy balance equations that govern the behavior of a catalytic membrane reactor with the following basic assumptions:

(1) isothermal or adiabatic conditions;
(2) plug flow on feed and sweep side of the catalytic membrane;
(3) no significant pressure drop along the feed and sweep side of the membrane.

Although such models have been successful in describing some of the available experimental data, they have not provided clear insight into many of the governing phenomena. For example, it has not been possible to clearly identify which fraction of the conversion comes from selective transport of species within the catalytic membrane, and which fraction is due to the lowering of the sum of partial pressures of the reactants and products on the sweep side of the membrane. By following a different approach and considering step by step the possible mechanisms that contribute to the membrane reactor's performance, we have been able to develop solutions based on dimensionless groups of parameters such as the Thiele Modulus and the Biot number which are often used in studying packed and fixed bed reactors. The following analysis of conversion in catalytic membranes allows intrinsic membrane properties (such as diffusivity differences) to be separated from extrinsic factors (such as differences in pressure on opposing sides of the membrane and dilution of products in a sweep gas which may be flowing on one side of the membrane).

In this paper a solution is presented that includes external mass transfer resistance effects and simulates diffusion within a single, catalyst-lined pore that ensures instantaneous reaction. Thus, local equilibrium is assumed to prevail throughout the pore. Imposing this rapid reaction condition allows a simple closed-form solution to be developed which reveals the importance of several phenomena. Although local thermodynamic equilibrium limits are never exceeded locally, the intrinsic properties of the membrane (such as permselectivity) can lead to enhanced conversion when extrinsic factors (such as dilution effects) are fixed. We define such enhancements as 'supra-equilibrium conversion'. It is also shown that external mass transfer resistance can significantly limit performance of a catalytic membrane. These effects can be minimized by operating with narrow dimensions and high velocities in the feed and permeate channels. However, in many bench-scale studies, these effects have been important because velocities were frequently set low in order to maximize overall conversion. Rigorous modeling of external mass transfer requires a multicomponent diffusion model, which has been incorporated into the theory.

In a future paper we will discuss asymptotic analyses that provide solutions to the governing equations when the reaction is not instantaneous.

## 2. Mathematical formulation and analysis

The key features of the one dimensional model simulating diffusion and instantaneous reaction in a catalyst-coated pore, are shown schematically in Fig. 1. A gaseous feed stream flowing at velocity,

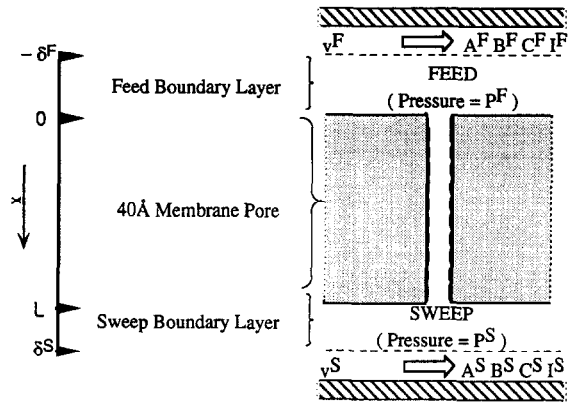


Fig. 1. Model based on a single pore in a catalytic membrane reactor.

$v^F$, in a channel on one side of the membrane contains a reactant ($A^F$), products ($B^F$ and $C^F$), and a molecular species ($I^F$) used as an inert sweep on the permeate side of the membrane. The superscript F denotes species on the feed side of the membrane. The molecular species must diffuse across a boundary layer of thickness $\delta^F$ to enter or leave the catalyst-lined pore structure. Within the catalyst-lined pore structure reaction is instantaneous and so local thermodynamic equilibrium prevails. The molecular species diffuse along the pore structure of length $L$ with diffusion coefficients $D_i$, where subscript $i$ denotes A, B, C or I. At the other side of the membrane, the species are transported by diffusion across a boundary layer of thickness $\delta^S$ into and out of a sweep stream flowing with a velocity $v^S$. The superscript S denotes species on the sweep side of the membrane. Pressures of the sweep and feed streams may be different. The thicknesses of the boundary layers, $\delta^S$ and $\delta^F$, are determined by the Laminar flow conditions on each side of the membrane.

Within the pore both reaction and diffusion determine the actual concentration profile of a species. The effects of reaction rate in the pore on concentration profiles are explicit in local steady-state material balances within the pore, which require:

$$D_A\frac{d^2[A]}{dx^2} = -D_B\frac{d^2[B]}{dx^2} = D_C\frac{d^2[C]}{dx^2} = r \qquad (1)$$

where $D_i$ is a diffusion coefficient, and $r$ the local rate of reaction. When reaction is instantaneous, $r$ is infinite and must be eliminated from Eq. (1) which can be regrouped in the form:

$$D_A\frac{d^2[A]}{dx} = -D_B\frac{d^2[B]}{dx} = 0 \qquad (2a)$$

$$D_B\frac{d^2[A]}{dx} = -D_C\frac{d^2[B]}{dx} = 0 \qquad (2b)$$

A further consequence of the instantaneous reaction rate is that the following equilibrium condition prevails everywhere within the pore structure:

$$\frac{K_p}{RT} = \frac{[B][C]}{[A]} \qquad (3)$$

where $K_p$ is the equilibrium constant, $R$ the ideal gas constant, and $T$ the temperature.

At the pore ends the fluxes of each species within the pore structure must match the fluxes of the species arriving from and entering the gas streams. Thus:

$$D_i\frac{d[i]}{dx} = -N_i^F \quad @x=0 \qquad (4a)$$

$$D_i\frac{d[i]}{dx} = -N_i^S \quad @x=L \qquad (4b)$$

where $N_i$ denotes species fluxes in an external boundary layer in the positive $x$ direction. Eqs. (4ab) are boundary conditions that any solution to Eqs. (2) must satisfy.

Because species I does not react within the pore, its flux and concentrations at the pore ends are related by:

$$N_I^F = N_I^S = D_I\frac{[I]^0 - [I]^L}{L} \qquad (5)$$

where superscripts 0 and $L$ denote respective conditions at $x=0$ and $x=L$.

Fluxes of species in the two boundary layers (of thicknesses $\delta^F$ and $\delta^S$, respectively) are properly calculated from the Stefan–Maxwell relations [11,12]:

$$\frac{dz_i^j}{dx}=\frac{RT}{P^j}\sum_{k=1}^{n}\frac{(N_k^j z_i^j - z_i^j N_i^j)}{D_{i,k}} \quad (6)$$

where $n=4$ is the number of components $i$; $k$ refers to species A, B, C, and I; $z$ denotes mole fraction; $j$=F or S; and $D_{ik}$ is a binary molecular diffusion coefficient.

Mathematical analysis based on Eq. (6), in which the species fluxes are implicit, is cumbersome. However, the analysis may be simplified [11] by replacing Eq. (6) with:

$$N_i^j=-\frac{D_i^j P^j\, dz_i^j}{RT\, dx} \quad (7)$$

where 'effective diffusion coefficients', '$D_i^j$' are defined by 'inversion' of Eq. (6) as follows:

$$\frac{1}{D_j^i}=\sum_{k=1}^{n}\frac{1}{D_{ij}}\left(z_i^j - z_k^j\frac{N_k^j}{N_i^j}\right) \quad (8)$$

The solution is necessarily iterative, with minor approximations introduced by insertion of arithmetic average mole fractions in Eq. (7).

Eq. (7) may be applied independently only $n-1$, i.e., three times in each boundary layer. However, there are four species fluxes in each boundary layer. The remaining two flux constraints are those imposed by the stoichiometry:

$$N_F^A - N_A^S = N_B^F + N_B^S = N_C^F + N_C^S \quad (9)$$

Total molar concentration in the gas boundary layers is determined by gas pressure and temperature assuming ideal gas behavior, i.e.:

$$[A]^j+[B]^j+[C]^j+[I]^j=\frac{P^j}{RT} \quad (j=F, S) \quad (10)$$

Insight into the underline physical phenomena may be obtained by transforming to the following set of dimensionless variables:

$$y=\frac{x}{L} \quad (11a)$$

$$i=\frac{[i]}{\frac{P^F}{RT}} \quad (11b)$$

Upon inserting Eqs. (11ab) into the above relationships, the following dimensionless groups evolve:

$$\theta_i=\frac{D_i}{D_B} \quad \text{where} \quad i=A, C \quad (12a)$$

$$\mu_i^j=\frac{D_i^j}{D_i\,\delta^j} \quad j=F, S \quad (12b)$$

$$\rho=\frac{P^S}{P^F} \quad (12c)$$

$$K=\frac{K_p}{P^F} \quad (12d)$$

$$\lambda=\frac{\delta^j}{L} \quad \text{where} \quad j=F, S \quad (12e)$$

where $\mu$ is the mass transfer Biot number and $K$ is a dimensionless equilibrium constant. Note that $\mu$ values evolve through the iterative determination of effective diffusion coefficients in the external boundary layers and that ratios of effective diffusion coefficients to boundary layer thicknesses are effective mass transfer coefficients.

Boundary layer thicknesses were estimated in Eq. (13) for a binary mixture of argon and ethane in laminar flow in a straight pipe, from available correlations [13] of Sherwood, Reynolds and Schmidt numbers:

$$\delta^j=\frac{d_h}{3.65+\dfrac{0.065\left(\dfrac{d_h}{L}\right)\left(\dfrac{d_h v^j}{D}\right)}{1+0.04\left[\left(\dfrac{d_h}{L}\right)\left(\dfrac{d_h v^j}{D}\right)\right]^{2/3}}} \text{ in cm} \quad (13)$$

where $d_h$ is a channel's hydraulic diameter, and $D$ a binary molecular diffusivity, which was calculated from the equation of Fuller and Giddings [12].

When Knudsen diffusion prevails in the membrane pore, $D_i$ takes the simple form:

$$D_i=\frac{\varepsilon D_{K,i}}{\tau} \text{ in cm}^2/\text{s} \quad (14)$$

where $\epsilon$ and $\tau$ are the porosity and tortuosity of the microporous membrane structure and $D_{K,i}$ is the Knudsen diffusion coefficient of species $i$ which is calculated from the kinetic theory of gases [12].

The remaining problem is algebraic and can be solved numerically if values of the dimensionless parameters in Eq. (12) and bulk compositions on each side of the membrane are specified. A numerical approach to solving for species fluxes and concentrations of species at each side of the membrane is described elsewhere [14].

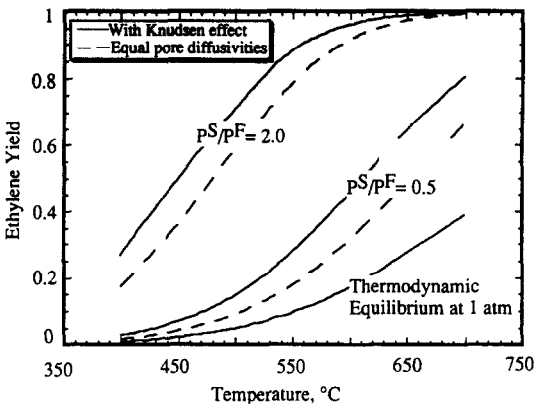


Fig. 2. Theoretical ethylene yield as function of temperature. Feed: 90% ethane/10% argon. Sweep: 100% argon at 1 atm. $\lambda = 360$.

## 3. Results and discussion

Our model has a differential reactor in the limiting case of complete diffusion control (very large Thiele modulus). To illustrate its use we consider the case of ethane dehydrogenation, which has been experimentally studied in the past with a catalytic membrane reactor. The reported studies [1–3] used an integral reactor in which gas compositions varied along the lengths of permeate and feed channels. Moreover Thiele Moduli were of order unity. Hence, quantitative comparison of predictions with the experimental results is precluded. Nonetheless, it is possible to make certain observations pertaining to the general behavior of such systems. Specifically, by examining the behavior of one pore of a membrane reactor it is possible to isolate the effects that can lead to equilibrium shift and are inherently due to the membrane selectivity. Membrane selectivity can be nullified by equating the diffusion coefficients of all species within the pore. The dimensionless parameters $\theta_i$ [see Eq. (12a)] will then be unity. Such an approach is essential for an understanding of the mechanisms that determine catalytic membrane reactor's performance.

To simulate ethylene dehydrogenation in a ca. 40 Å pore diameter $\gamma$-$Al_2O_3$ membrane, pore diffusivities were set to vary inversely with square root of molecular weight. The reaction equilibrium constant was reported elsewhere [3] to be:

$$K_p = 1.096\ 10^7 \exp\left(\frac{34.26}{RT}\right) \text{atm} \qquad (15)$$

where $R$ in kcal/mole $K$, and $T$ is the temperature in K.

Fig. 2 shows ethylene yield calculated as a function of temperature, with 90% ethane/10% argon feed, and a pure argon sweep gas at a fixed pressure of 1 atm, and both $\lambda$ values = 380. 'Yield' is defined by Eq. (16) as the ratio of total flux of ethylene leaving the pore (at both ends) to the flux of ethane into the pore from the feed stream (the difference being the flux of unreacted ethane into the sweep stream).

$$\text{Yield} = \frac{N_B^F + N_B^S}{N_A^F} \qquad (16)$$

The lowest curve depicts equilibrium conversion calculated for a closed system at 1 atm (i.e., maximal conversions at that pressure in a conventional reactor without in situ product removal). Theoretical results were calculated for the pressure ratio, $\rho = 0.5$ (i.e., a feed pressure of 2 atm) and $\rho = 2$ (a feed pressure of 0.5 atm). Comparison was made of results calculated assuming that (a) pore diffusivities varied inversely with square root of molecular weight (Knudsen diffusion), and (b) all diffusivities equalled the Knudsen value for ethane (broken curves).

Notably, with either basis for calculating diffusivities, the theoretical curves in Fig. 2 depicting catalytic membrane performance lie

substantially above the thermodynamically limiting curve for a closed system. Three different effects contribute to this supra-equilibrium conversion. The first two are attributable to le Chatelier's principle, yielding enhanced conversion when the feed and products are diluted with the sweep gas and when reducing partial pressures on both feed and sweep side of the membrane. The third is due to the permselectivity of the membrane which selectively transports hydrogen, shifting the equilibrium within the pore structure. These three effects are easily separated by the model because the first two effect do not require the membrane to be permselective, while the third only occurs with a permselective membrane. The relative magnitudes of these effects are apparent in Fig. 3. The solid curves lie only slightly above the corresponding dashed ones, and the curves for $\rho=2$ are well above those for $\rho=0.5$. At least under the conditions modeled here, 'supra-equilibrium' conversion is primarily attributable to le Chatelier's principle, i.e., the effects of dilution with sweep gas and reduced pressure. There is substantial promotion of conversion even when the feed gas is at twice the base case pressure (note that higher fluxes of ethane into the pore associated with higher pressure driving forces, do not in and of themselves enhance yield as defined above). There is, clearly, additional promotion of ethane conversion due to the permselective properties of the membrane (selective product removal by permeation). However, it is a relatively small effect.

External mass transfer resistances were also taken into account in the theoretical model and were represented in the Biot numbers ($\mu$). Since the effective bulk gas molecular diffusion coefficients based on Eq. (8) were determined iteratively, graphical results refer only to preset values of $\lambda=\delta/L$, the ratio of boundary layer thickness and effective pore length [see Eq. (12e)]. Although $\lambda$ is quite large compared to unity, this is offset by a large ratio of effective bulk to Knudsen diffusivities, and so the external mass transfer resistance was significant but not dominant. Its influence is depicted in Fig. 3 where ethylene

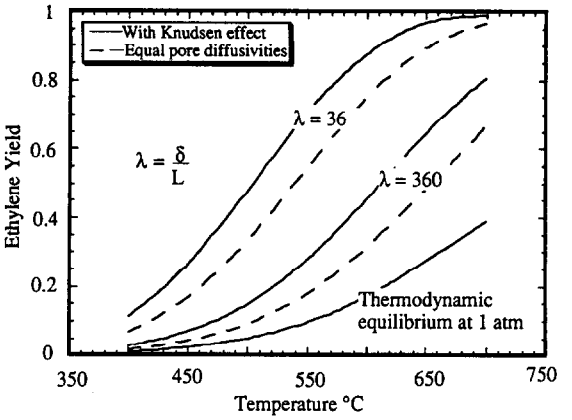


Fig. 3. Ethylene yield vs. temperature at two different $\lambda$ values, with and without membrane permselectivity. Feed: 90% ethane/10% argon at 0.5 atm. Sweep: 100% argon at 1 atm.

yield is plotted as a function of temperature for different $\lambda$ values. The results are again plotted with and without assumed permselectivity. Lower $\lambda$ implies smaller external mass transport effects. A typical asymmetric alumina membrane has a final thin (ca. 5 $\mu$m) microporous coating of $\gamma$-$Al_2O_3$ that provides Knudsen selectivity. Previous investigations (3) operated at sufficiently low gas velocities ($v^j$) that Eq. (13) reduces to:

$$\delta^j = d_h/3.65 \qquad (17)$$

which yields a typical boundary layer thickness of 1 mm. Fig. 3 suggests that at such $\lambda$ values the effect of external mass transport is quite significant. Its effect was investigated further by calculating ethylene yield isotherms over a complete range of $\lambda$ values see Fig. 4. In the asymptotic

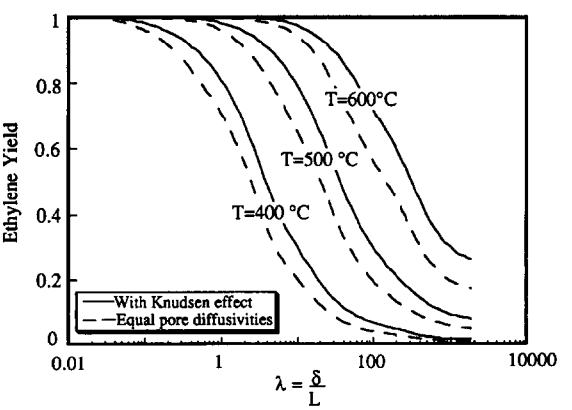


Fig. 4. Ethylene yield vs. $\lambda$ at three different temperatures with and without membrane permselectivity. Feed: 90% ethane/10% argon at 0.5 atm. Sweep: 100% argon at 1 atm.

limit of negligible external resistance ($\lambda \rightarrow 0$), yield is 100%. Correspondingly, at very large $\lambda$ values yield goes to zero.

From the analysis of the results the following conclusions can be made:

(1) trans-membrane pressure drop is a very important operational advantage of asymmetric membranes that results in supra-equilibrium conversions;

(2) external mass transfer resistance can significantly effect the performance of high flux asymmetric membranes.

The conditions and the membrane configurations described here are typical of laboratory membrane reactors that have been used for olefin dehydrogenation. A comparison of the theoretical results presented here and experimental results obtained with an asymmetric pressure drop membrane reactor will be discussed in a future communication [14].

## References

[1] Y.M. Sun and S.J. Khang, Ind. Eng. Chem. Res., 27 (1988) 1136.
[2] Y.M. Sun and S.J. Khang, Ind. Eng. Chem. Res., 29 (1990) 232.
[3] A.M. Champagnie, T.T. Tsotsis, R.G. Minet and I.A. Webster, 45 (1990) 2423.
[4] V.T. Zaspalis, W. van Praag, K. Keizer, J.G. van Ommen, J.R.H. Ross and A.J. Burggraaf, Appl. Catal., 74 (1991) 205.
[5] V.T. Zaspalis, W. van Praag, K. Keizer, J.G. van Ommen, J.R.H. Ross and A.J. Burggraaf, Appl. Catal., 74 (1991) 223.
[6] V.T. Zaspalis, W. Van Praag, K. Keizer, J.G. van Ommen, J.R.H. Ross and A.J. Burggraaf, Appl. Catal., 74 (1991) 235.
[7] V.T. Zaspalis, W. van Praag, K. Keizer, J.G. van Ommen, J.R.H. Ross and A.J. Burggraaf, Appl. Catal., 74 (1991) 223.
[8] J.C.S. Wu and P.K.T. Liu, Ind. Eng. Chem. Res., 31 (1992) 322.
[9] M.E. Olbrich and J.H. Kolts, AIChE Spring National Meeting, New Orleans, LA (1986).
[10] J. Karger and D.M. Ruthven, Diffusion in Zeolites, John Wiley, New York, (1992).
[11] Hsu and Bird, AIChE J., 6 (3) (1960) 516.
[12] R.C. Reid, J.M. Prausnitz and T.K. Sherwood, The Properties Of Gases And Liquids, McGraw-Hill, New York (1977).
[13] D.K. Edwards, V.E. Denny and V.F. Mills, Transfer Processes, McGraw-Hill, New York (1979).
[14] V. Papavassiliou, Ph.D. Thesis, Tufts University (1995).